ICES Journal of Marine Science

ICES Journal of Marine Science (2013), 70(7), 1451–1459. doi:10.1093/icesjms/fst095

Boarfish (*Capros aper*) target strength modelled from magnetic resonance imaging (MRI) scans of its swimbladder

Sascha M. M. Fässler[1]*, Ciaran O'Donnell[2], and J. M. Jech[3]

[1]*Wageningen Institute for Marine Resources and Ecosystem Studies (IMARES), PO Box 68, 1970 AB Ijmuiden, The Netherlands*

[2]*Marine Institute, Rinville, Oranmore, Co.Galway, Ireland*

[3]*National Oceanic and Atmospheric Administration, Northeast Fisheries Science Center, 166 Water Street, Woods Hole, MA, USA*

**Corresponding author: tel: +31 317 487474; fax: +31 317 487326; e-mail: sascha.fassler@wur.nl*

Fässler, S. M. M., O'Donnell, C., and Jech, J.M. 2013. Boarfish (*Capros aper*) target strength modelled from magnetic resonance imaging (MRI) scans of its swimbladder. – ICES Journal of Marine Science, 70: 1451–1459.

Received 28 September 2012; accepted 28 May 2013; advance access publication 6 August 2013.

Boarfish (*Capros aper*) abundance has increased dramatically in the Northeast Atlantic from the early 1970s after successive years of good recruitment attributed to an increase in sea surface temperature. Due to increased commercial fishing over recent years, an acoustic boarfish survey funded by the Killybegs Fishermen's Organisation was initiated by the Marine Institute to establish a baseline for the future management of this stock. In the absence of any species-specific boarfish target strength (*TS*), acoustic backscatter was estimated by a Kirchhoff-ray mode model using reconstructed three-dimensional swimbladder shapes which were computed from magnetic resonance imaging scans of whole fish. The model predicted *TS* as a function of size, fish tilt angle, and operating frequency. Standardized directivity patterns revealed the increasing importance of changes in the inclination of the dorsal swimbladder surface at higher frequencies (120 and 200 kHz) and a less directive response at lower frequencies (18 and 38 kHz). The model predicted a *TS*-to-total fish length relationship of $TS = 20\log_{10}(L) - 66.2$. The intercept is ~1 dB higher than in the general physoclist relationship, potentially reflecting the bulky nature of the boarfish swimbladder with its relatively large circumference.

Keywords: acoustic survey, boarfish, Kirchhoff-ray mode (KRM), stock assessment, target strength.

Introduction

Acoustic survey techniques are used widely to provide data on schooling pelagic fish that form distinct aggregations in midwater (Simmonds and MacLennan, 2005). Collected acoustic data will yield fish area density values (nautical area scattering coefficient, s_A, in m^2 nautical $mile^{-2}$) along transects (MacLennan *et al.*, 2002). Conversion of acoustic density to fish abundance is done by use of a species-specific target strength (*TS*) that describes the sound-scattering potential of one individual fish. Abundance estimation techniques from acoustic survey data rely on relationships between *TS* and fish length (*L*) of the form $TS = m\log_{10}(L) + b$. Commonly, the slope parameter *m* is fixed to the theoretical value of 20, indicating a proportional relationship between the square of the fish length and acoustic backscatter (McClatchie *et al.*, 2003), and a species-specific value for the intercept parameter *b* is used (Foote, 1987). Currently, *TS*–*L* relationships are available for many important commercial species or species groups whose stock sizes are regularly estimated by acoustic surveys. *TS*–*L* relationships are usually estimated based on the *ex situ* measurements of immobilized or dead fish, fish in cages, or those observed *in situ* in their natural habitat. The majority of the currently accepted and practically applied relationships to convert fish length into *TS* are based on extensive *in situ* datasets. Such measurements have been deemed preferable and most representative for deriving species-specific *TS*–*L* relationships because they are obtained from fish free to behave as they would during an acoustic survey (Foote, 1987; Simmonds and MacLennan, 2005). Still, there are basic limitations associated with *in situ* measurements to do with practical difficulties that are common for remote sensing approaches. These involve: (i) multiple target detection (Soule *et al.*, 1995), (ii) representativeness of the acoustically detected fish targets (MacLennan and Menz, 1996), and (iii) correct collection and representativeness of biological samples (MacLennan, 1992). Such limitations and recent advances in computing power have been driving the development and use of sound-scattering models based on morphological and physical data of fish (Horne *et al.*, 2000; Foote and Francis, 2002; Fässler *et al.*, 2009). Such models have the advantage that, given appropriate input data, they can produce reliable estimates of mean *TS* in the

absence of any other available measurements (Demer and Conti, 2005). This work is one of the first to describe a model-based *TS*–*L* relationship for a commercially fished and acoustically monitored species for which no empirical estimates of *TS* exist.

From the early 1970s onwards, the abundance of boarfish (*Capros aper*) in the Northeast Atlantic has increased dramatically after successive years of good recruitment attributed to an increase in sea surface temperature during the spawning season (Blanchard and Vandermeirsch, 2005). The growth in boarfish population resulted in this species developing from an unwelcome incidental bycatch to a large-scale dedicated international pelagic fishery with landings more than 137 500 t in 2010 (ICES, 2011). During the spawning period between June and August, this pelagic species forms large, high-density spawning aggregations on the continental shelf off the west and southwest coast of Ireland. The boarfish in this area are predominantly distributed at water depths of 70–140 m; however, individual high-density schools can occur within the first 50 m below the surface. High-density aggregations are most abundant during daylight hours when spawning activity is more intense, while during the night boarfish form diffuse layers close to the seabed (O'Donnell *et al.*, 2012). Outside of the spawning period boarfish move eastwards away from the shelf edge to a more on-shelf distribution where they are known to form large overwintering aggregations. In 2011, the first acoustic survey funded by the Killybegs Fishermen's Organisation (Killybegs, Co. Donegal, Ireland) was carried out to determine the spatial distribution and abundance of the spawning aggregations (O'Donnell *et al.*, 2011). At the time, no species-specific *TS*–*L* relationship was available for boarfish. Basic knowledge of their main sound-scattering organ the swimbladder was also lacking, except that it was "relatively large" (Fish, 1948) and of the physoclistous type (Marshall, 1960). Preliminary estimates of abundance and biomass of the stock, therefore, had to be based on the use of a range of "candidate" *TS*–*L* relationships previously determined for gadoids, Atlantic herring, and snipefish (*Macroramphosus* spp.). These resulted in up to >20-fold differences in estimated total-stock biomass. To reduce this uncertainty, an effort to generate a boarfish-specific *TS*–*L* relationship was initiated.

To estimate a length-dependent relationship of mean *TS* for boarfish, swimbladders were scanned in a magnetic resonance imaging (MRI) scanner to extract three-dimensional information of their shapes and sizes. The Kirchhoff-ray mode (KRM) model (Clay and Horne, 1994) was used to compute backscattering cross sectional areas (σ_{bs}, in m^2; Clay and Medwin, 1977) of each swimbladder as a function of frequency, size, and tilt angle. Angle averaged *TS* were used to derive a fish-orientation weighted *TS*-*L* relationship. Frequency-dependent backscatter estimates were used to produce an expected relative frequency response of boarfish (Korneliussen and Ona, 2003). Knowledge of the species-specific relative frequency response will facilitate categorization and species identification from acoustic multifrequency data.

Material and methods

Fish sample collection

Boarfish were collected on board the commercial vessel FV "Felucca" during the dedicated boarfish acoustic survey in July 2011. A midwater trawl with 90 m × 45 m opening and 20 mm mesh size in the codend liner was used during the survey to collect samples corresponding to the recorded echotraces for species identification and biological condition (length, weight, age, sex, and maturity; O'Donnell *et al.*, 2011). Time between shooting and recovering the net ranged from 31 to 69 min. Individuals used in this study were only collected from trawls targeting schools at the upper depth distribution limits observed (<40 m). This was to ensure that the depth-adapted physoclistous boarfish swimbladders were minimally affected by the catching process. According to Blaxter and Batty (1990), a physoclist will require ~75 min to regain neutral buoyancy after a 50-m ascent. Based on these estimates, the sampled boarfish had sufficient time to adjust their swimbladders to changing pressure conditions after being hauled slowly to the sea surface and before being frozen. For the backscatter model to derive reliable *TS* estimates from the boarfish swimbladders, they should ideally be intact, non-collapsed, and inflated to a depth-adapted state, in which the fish are neutrally buoyant. Harden Jones and Scholes (1981) suggested that fish will be neutrally buoyant at the upper limit of their diurnal vertical range, and this was assumed to be the case for the boarfish swimbladders at depths from which the samples were taken. Forty-three specimens covering the size range 12–17.5 cm and weighing 22–116 g were collected from the selected trawl catches. Sample selection was done under the condition of showing no external damage. Each sample was laid on a grease-proof paper and left to freeze for a period of 48 h at −20°C. Thereafter, fish were put in individual labelled sampling bags and stored frozen.

X-ray and MRI

To confirm that the swimbladders of the boarfish samples remained intact after capture and handling, at least one individual from each 0.5 cm length class ($n = 14$) was selected for radiography. The frozen samples were defrosted slowly at 4°C for 24 h, to avoid changes in swimbladder shape (Yasuma *et al.*, 2003, 2010; Peña and Foote, 2008), before being transported in an insulated cool box. Each individual was radiographed (i.e. X-rayed) in the lateral and dorsoventral position. This was carried out using a BCF 10040HF X-ray generator (BCF Technology Ltd, Ireland) over a Kodak CR phosphate cassette-based acquisition plate.

After confirming intactness of their swimbladders, the X-rayed boarfish samples were taken for MRI together with an additional 18 boarfish selected across the size range (total of 32 fish samples). Before scanning, these additional samples were also defrosted at 4°C for 24 h and transported in a refrigerated state to the scanning facility. MR images of transverse sections of the fish were collected using an Esaote E-Scan XQ (model: 9700019006, ESAOTE S.p.A, Italy), which is a low open-field scanner with a permanent magnet and field strength of 0.2 T. Compared with other scanners used in similar investigations (Peña and Foote, 2008; Fässler *et al.*, 2009), the scanner used here had a lower field strength. However, the resulting spatial resolution (Table 1) was adequate for swimbladder extraction. A 19-cm diameter head coil with a length of 24 cm was used during scanning. To facilitate scanning, a polyurethane foam cradle was used to stabilize and contain up to four horizontally oriented fish during a single acquisition (Figure 1). A number of initial test scans was carried out to determine the optimum MR parameters (Table 1). Image acquisition parameters were chosen to optimize the compromise between spatial imaging resolution and size of the imaging region (*sensu* Peña and Foote, 2008), while accomplishing all scanning sequences of the boarfish samples within the available 5-h time slot. Swimbladder scans were acquired in the axial plane. In all, 11 scan series were carried out on the boarfish samples, resulting in a total of 594 individual slices. Digital images of each slice were generated and exported from the scanner

Table 1. Sample details and MRI scan parameters.

MRI attribute	Axial sequence
Pixel size (mm)	0.55 – 0.78
Slice thickness (mm)	1.9 – 2.5
Samples per pixel	1
Acquisition type	Turbo three-dimensional
Repetition time (ms)	38.0 – 41.0
Echo time (ms)	16.0 – 18.0
Acquisition time (min:s)	9:34 – 12:50
Space between slices (mm)	1.9 – 2.5
Number of slices	52 – 58
Number of averages	3
Image rows × columns	256 × 256

Figure 1. MRI coil containing the rubber foam cradle and boarfish samples.

in the Digital Imaging and Communications Medicine (DICOM) file format.

Bladder reconstruction and *TS* modelling

An image processing and programming routine was developed using MATLAB (version 7.0; The MathWorks Inc., MA, USA) with the Image Processing Toolbox™ to reconstruct three-dimensional representations of the swimbladders from the MR image slices (Fässler, 2010). The high image contrast between the gas-filled swimbladder and surrounding tissue enabled the accurate assessment of the swimbladder boundaries from the MR images (Figure 2). Due to the presence of prominent and strong X-ray-absorbing spines in the boarfish dorsal fins, adequate tracing of swimbladder boundaries was impossible from dorsal X-ray images alone. The MATLAB routine allowed the swimbladder boundaries to be defined on a slice-by-slice basis by applying a threshold value in the colour scale to extract the dark pixels (in-plane, two-dimensional elements) characteristic of the gas-filled swimbladder structure while excluding the lighter pixels denoting the surrounding bone and tissue. The swimbladder of each boarfish sample was then built up from its individual cross sections using all individual image slices of the combined sequence. In-plane pixel resolution and the distance between slices were fixed for each scan but ranged from 0.55 to 0.78 mm and 1.9 to 2.5 mm, respectively, between different scans (Table 1). With these data, the swimbladder volume was calculated by adding all voxels (three-dimensional

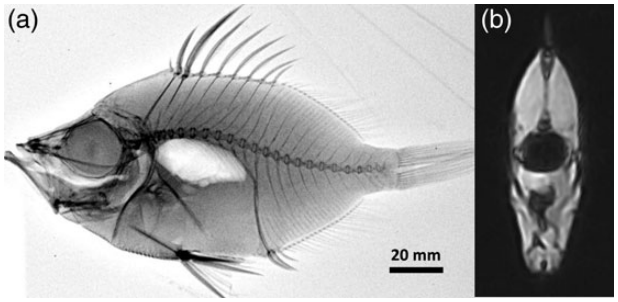

Figure 2. Lateral X-ray (a) and axial MRI section from the central portion (b) of a 175-mm boarfish sample used for *TS* modelling. The swimbladder corresponds to the respective white (X-ray) and dark (MRI) shape in the centre of the fish body.

elements) for each swimbladder. Tracing the accuracy of the swimbladder was improved (cf. Peña and Foote, 2008) by applying the "smooth3" three-dimensional object smoothing function with a Gaussian convolution kernel of size [1 1 1] and 0.65 s.d. in the MATLAB routine. A three-dimensional object corresponding to the smoothed swimbladder was then created using the "patch" function in MATLAB, and a mesh defining the surface was reconstructed based on the x, y, and z coordinates of the object boundaries (Figure 3). Since the MRI scans focused on the swimbladders, true shapes of the fish body could not be traced and reconstructed from the scanning slices. Instead, fish body dimensions were traced from the silhouettes of lateral and dorsal aspect digital images of one of the boarfish samples and linearly scaled as a function of length for use with the other individuals (cf. Horne *et al.*, 2000; Gauthier and Horne, 2004).

Acoustic backscatter of the boarfish was modelled using the three-dimensional swimbladder shapes and applying the KRM approximation (Clay and Horne, 1994; Horne and Jech, 1999). The KRM approximates scattering objects as a contiguous series of finite cylinders and at the frequencies and fish lengths used in this study uses the Kirchhoff approximation (Medwin and Clay, 1998) to predict σ_{bs} as a function of size, frequency, and orientation relative to the transducer. The fish body was represented as a set of fluid-filled cylinders surrounding the gas-filled cylinder sections of the swimbladder. Total fish backscatter was calculated as the coherent sum of both swimbladder and fish body cylindrical elements (Clay and Horne, 1994). During silhouette tracing, the fish body axis was at horizontal orientation. Individual cylinder components of the fish body and swimbladder were generated based on the height and width of the respective scattering bodies along the main axis directions in the horizontal plane, from the snout to the tip of the caudal peduncle (Horne *et al.*, 2000). Diameters of the individual cylinder sections were obtained from the means of their respective widths and heights (Reeder *et al.*, 2004). The swimbladder was assumed to be gas-filled with a density of 13.62 kg m^{-3}. This value reflects pressure conditions at 100-m water depth, where boarfish are typically encountered during surveys west of Ireland. The fish body component was assumed to be fluid-filled with a slightly higher density (1070 kg m^{-3}) than the surrounding seawater (1027 kg m^{-3}). Speed of sound in seawater, fish body, and swimbladder were 1500, 1570, and 340 m s^{-1}, respectively.

To derive a tilt angle-averaged mean *TS*-to-total fish length relationship [$TS = 10 \log_{10}(\sigma_{bs})$; MacLennan *et al.*, 2002], σ_{bs} were predicted for each individual boarfish specimen as a function of total fish

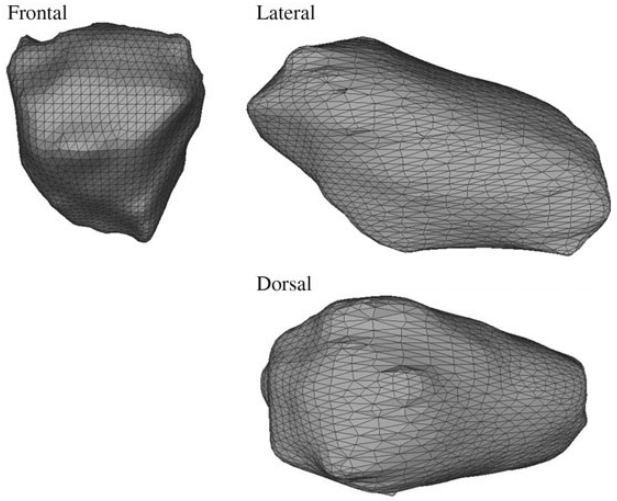

Figure 3. Three-dimensional reconstruction of the swimbladder of a 175-mm boarfish, represented as a wire frame composed of triangles shown at different aspects. The swimbladder has a length of 37 mm and all representations are at the same scale.

length (L) and frequency (f) over tilt angles ranging from 40° to 140° from dorsal aspect, where 90° is normal dorsal incidence. Dorsal-aspect σ_{bs} were subsequently averaged over 100 000 samples of normally distributed tilt angles (θ) then converted into logarithmic TS. The tilt angle distribution used, $\theta \sim N(88.5^\circ, 14.5^\circ)$, is based on various tilt angle distributions previously measured and used for several pelagic species with swimbladders (McClatchie *et al.*, 1996; Gauthier and Horne, 2004): capelin (Carscadden and Miller, 1980), Atlantic herring (Buerkele, 1983; Foote, 1983; Ona, 1984, 2001), and cod (Olsen, 1971). For comparison purposes, a range of additional mean TS–L relationships were calculated based on different Gaussian distributions of tilt angle with means of 90° and varying s.d. Parameters of TS–L relationships were derived by fitting a linear regression to the modelled tilt-averaged mean TS at 38 kHz. Apart from the standard frequency used in acoustic surveys for fish (38 kHz), backscatter was also estimated for a range of other commonly used frequencies (18, 70, 120, and 200 kHz). Comparisons of backscatter among frequencies were done by normalizing the modelled σ_{bs} values for all boarfish samples (n) across frequencies and angles relative to the maximum value observed. Normalized σ_{bs} were then averaged for every tilt angle and frequency combination and presented in the logarithmic scale as normalized TS relative to the maximum value observed among all frequencies:

$$\widehat{TS}(f, \theta) = 10 \log_{10}\left\{\frac{1}{n}\frac{\sum_{s=1}^{n} \sigma_{bs}(f, \theta)_s}{\max[\sigma_{bs}(f, \theta)]}\right\}. \quad (1)$$

Backscatter at different frequencies was compared by the use of the dimensionless relative frequency response [$r(f)$; Korneliussen and Ona, 2003]. These were computed for each individual boarfish sample (s) and averaged over f to give mean values:

$$\overline{r(f)} = \frac{1}{n}\frac{\sum_{s=1}^{n} \sigma_{bs}(f)_s}{\sigma_{bs}(f_{38\,kHz})_s}. \quad (2)$$

Results

Three-dimensional swimbladder shapes

Of the 32 scanned fish swimbladders, 24 were deemed intact and suitable for three-dimensional shape reconstruction. These swimbladders showed no signs of abnormal expansion or collapse and could be traced with ease using the MATLAB routine. The measured volume of the swimbladders relative to that of the fish body was on average 5.2% (s.d. = 1.9%), which is in agreement with the theoretical value for neutrally buoyant marine fish (Harden Jones and Marshall, 1953). Boarfish swimbladder shapes appeared generally shortened with similar maximum height (mean, 11.0 mm; s.d., 3.2 mm) and width (mean, 12.1 mm; s.d., 2.7 mm). Swimbladder lengths ranged from 13 to 37 mm and ratios of swimbladder to fish total length had a mean and s.d. of 0.18 and 0.02, respectively. Figure 3 illustrates a representative boarfish swimbladder from the examined samples: the dorsal aspect displays a pear shape with the width varying marginally along the main axis and the maximum extent found in the medial portion of the bladder. The lateral aspect shows a triangular shape extending from the anterior point towards about one-third along the axis length with the viscera of the fish occupying the space in the abdominal cavity below the swimbladder (Figure 2a). Beyond that point, the ventral surface of the swimbladder remains horizontal, whereas the dorsal surface follows the vertebral column down towards the posterior end. The inclination angle of the dorsal swimbladder surface relative to the fish axis was measured on the sagittal X-ray images ($n = 14$). The fish axis was defined as the imaginary line between the root of the tail and the tip of the upper jaw (Peña and Foote, 2008). Measurements of that angle revealed a mean value of 13.0° with s.d. of 2.5°.

Backscatter modelling

Figure 4 shows the normalized mean TS [Equation (1)] over the tilt angle range used for all observed boarfish samples at frequencies (18, 38, 70, 120, and 200 kHz). The directivity pattern, or influence of tilt on the estimated TS, was least affected at the lowest frequency (18 kHz) with just 3.0–4.5 dB difference between the maximum TS value and the TS estimated at the edges of the angle range (40° and 140°). The directivity increased with increasing frequency and at 200 kHz, differences between maximum TS and the lowest values observed within the angle range presented was ~16 dB. Directivity patterns were more symmetric at lower frequencies (18 and 38 kHz), whereas at 70, 120, and 200 kHz, a secondary peak or plateau feature could be observed at head-up angles between +10° and +30° relative to horizontal aspect (Figure 4). Similarly, maximum TS values occurred at 92.0° for 18 kHz and towards head-down angles for successively higher frequencies: 81.0° at 38 kHz, 80.0° at 70 kHz, 76.2° at 120 kHz, and 76° at 200 kHz. These tilt angles of maximum TS at successively higher frequencies were in agreement with the mean measured inclination angle between the dorsal swimbladder surface and the fish axis (corresponding to a mean tilt of 77.0°). Highest maximum mean TS was estimated at 38 kHz with slightly lower values at 70, 120, and 200 kHz (−0.2, −0.2, and −0.5 dB, respectively), and 1.2 dB lower at 18 kHz.

The tilt-averaged backscattering cross section at the five frequencies analysed showed a decreasing relative frequency response [$r(f)$; Equation (2)] with increasing frequency (Figure 5). $r(f)$ at 120 and 200 kHz gave similar values of 0.71 and 0.68, respectively. Compared with these, $r(f)$ values at 18 and 70 kHz were slightly higher at 0.90 and 0.85. 95% confidence intervals around these mean values had similar widths ranging between 0.13 (70 kHz)

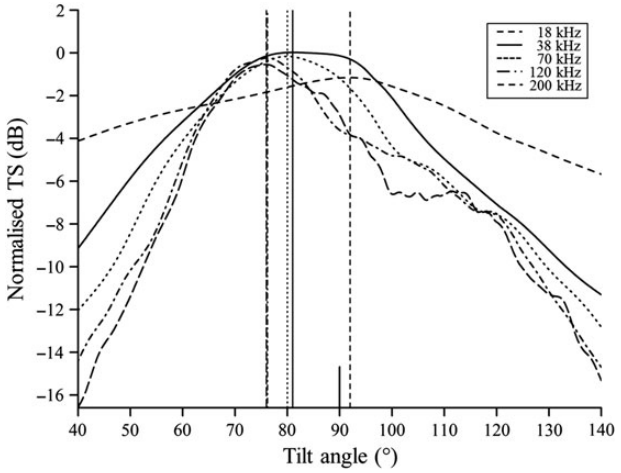

Figure 4. Normalized mean *TS* of 24 boarfish at typical frequencies used in fisheries acoustics (18, 38, 70, 120, and 200 kHz) as a function of tilt angle, predicted by the KRM approximation. Dorsal aspect is at an angle of 90°. Head-down and head-up orientations are indicated at angles $<90°$ and $>90°$, respectively. Mean *TS*s were normalized by the maximum TS among all five frequencies. Vertical lines designate the tilt angle of maximum *TS* at a given frequency indicated by the respective line types used.

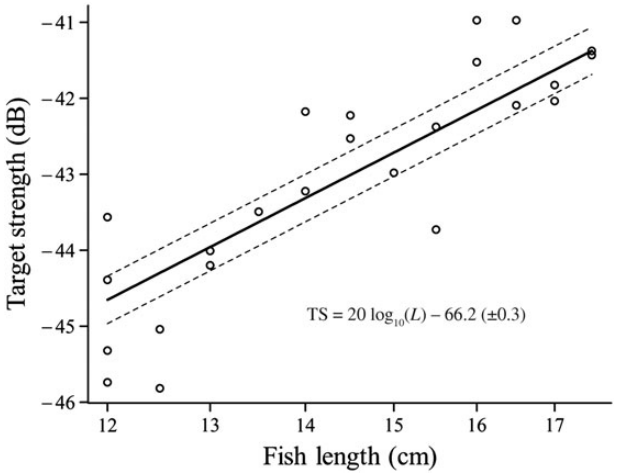

Figure 6. The mean *TS* function of total fish length modelled by the KRM approximation at 38 kHz. *TS*s were averaged over a normally orientated tilt angle distribution with mean 88.5° (dorsal-aspect) and s.d. 14.5°. Regression equation of the standard form $[TS = 20 \log_{10}(L) + b_{20}]$ and 95% confidence interval around the estimated intercept is given.

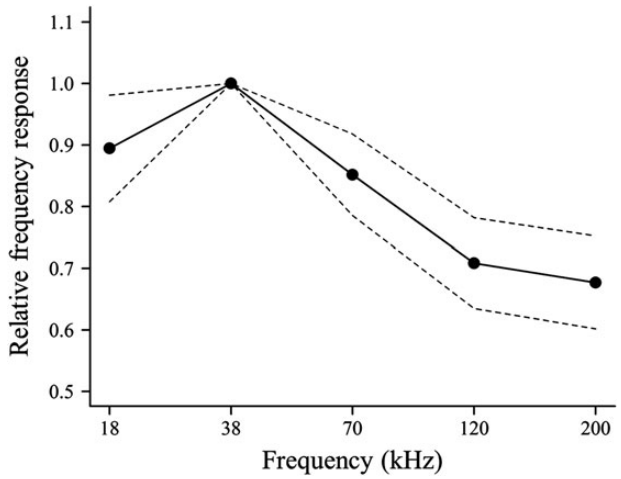

Figure 5. Frequency-dependent backscattering cross section (σ_{bs}) of 24 boarfish predicted by the KRM approximation at typical frequencies used in fisheries acoustics (18, 38, 70, 120, and 200 kHz) relative to the backscatter at 38 kHz (i.e. relative frequency response). Filled dots represent the mean values with 95% confidence intervals (dashed lines).

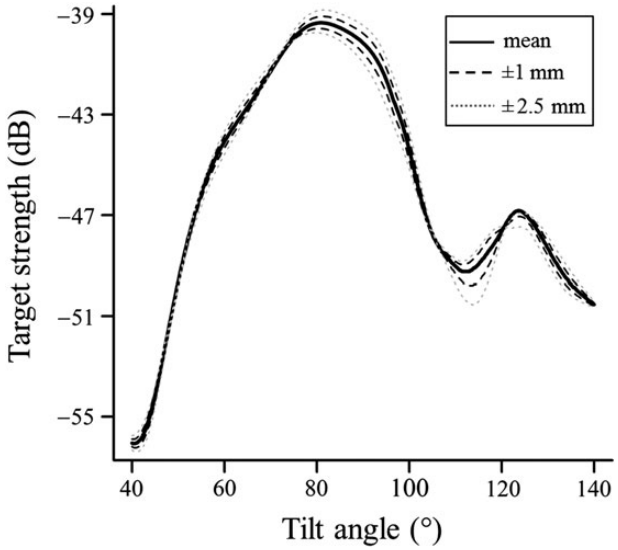

Figure 7. The mean *TS* of a 175-mm boarfish at 38 kHz as a function of tilt angle, predicted by the KRM approximation. Dorsal aspect is at an angle of 90° and the different lines represent calculations based on varying fish body dimensions relative to the mean size.

and 0.17 (18 kHz). These attributes could generally be linked to the observed shift in maximum backscatter towards 10–15° head-down tilt orientation with increasing frequency (Figures 4 and 5). This resulted in lower mean backscatter at progressively higher frequencies relative to 38 kHz under the assumption of the near-horizontal tilt angle distribution used. Lower relative frequencies at 18 kHz were due to the lower absolute value of maximum *TS* at that frequency relative to 38 kHz (Figure 4).

The regression analysis between tilt-averaged *TS* and *L* in the standard form assuming a fixed slope of 20 at 38 kHz revealed a mean intercept value of -66.2 (± 0.3) dB (Figure 6). To test the sensitivity of the fish body contribution to the estimated total fish backscatter, *TS* of a 175-mm boarfish specimen was estimated for varying dimensions of the fish body cylinder components. These ranged from $+2.5$ to -2.5 mm of the scaled fish body contours, effectively representing up to 5 mm differences in body dimensions (Figure 7). The mean *TS* averaged over angles $\theta \sim N(88.5°, 14.5°)$ varied by up to 0.3 dB between the mean fish body dimension and the deviations.

The regression parameter b_{20} was also estimated assuming tilt angle distributions with means at horizontal orientation (90°) but

Table 2. Regression analyses of tilt angle averaged mean *TS* at 38 kHz vs. total fish length *L* (cm) for 24 boarfish.

Tilt angle (°)		$TS = m \log_{10}(L) + b$			$TS = 20 \log_{10}(L) + b_{20}$	
Mean	**s.d.**	***m***	***b***	**s.e.**	b_{20}	**s.e.**
90	5	25.8	−72.2	0.8	−65.4	0.9
90	10	24.0	−70.5	0.8	−65.9	0.8
90	15	22.1	−68.7	0.7	−66.4	0.7
90	20	21.0	−68.1	0.7	−66.9	0.7
88.5	14.5	22.6	−69.3	0.7	−66.2	0.7

Parameters *m* and *b* are the respective slope and the intercept in the general relationship $TS = m \log_{10} L + b$, and b_{20} is the intercept in the same relationship with a slope (*m*) fixed at 20. The standard error of the regression (residual standard error) is designated as s.e.

with various different s.d. chosen close to values previously observed, estimated, or used, i.e. $N(90^\circ, 5^\circ)$ for saithe (*Pollachius virens*; Foote and Ona, 1987), $N(90^\circ, 10^\circ)$ for Atlantic herring (Buerkele, 1983), $N(90^\circ, 15^\circ)$ for Atlantic herring (Foote, 1983) or Atlantic cod (Olsen, 1971), and $N(90^\circ, 20^\circ)$ for capelin (*Mallotus villosus*; Carscadden and Miller, 1980). These results showed that the intercept decreased with increasing width of tilt angle distribution for $N(90^\circ, 5^\circ)$ and $N(90^\circ, 20^\circ)$, from −65.4 to −66.9 dB (Table 2). The *TS*–*L* relationship for $N(88.5^\circ, 14.5^\circ)$ was not significantly different from those assuming tilt angle distributions with either $N(90^\circ, 10^\circ)$ or $N(90^\circ, 15^\circ)$ (multiple linear regression, *F*-ratio = 2.72, $p = 0.07$). Smoothing of swimbladder surfaces during the extraction and reconstruction process could have caused a bias in estimated backscatter (Jech and Horne, 1998). To investigate the sensitivity of this procedure on the *TS*–*L* relationship, regressions were also fitted to *TS* estimates of non-smoothed swimbladders averaged over tilt angles $\theta \sim N(88.5^\circ, 14.5^\circ)$. Although slightly higher [$b_{20} = -66.0\ (\pm 0.5)$], the estimated intercept did not differ significantly from the one based on smoothed swimbladders. When an arbitrary slope was assumed, the slope decreased from 25.8 at the narrowest tilt angle distribution $N(90^\circ, 5^\circ)$ to 21.0 at the widest distribution of tilt angle $N(90^\circ, 20^\circ)$ (Table 2). The intercept correspondingly increased from −72.2 to −68.1 dB.

Discussion

Radiographic methods have been applied extensively to describe swimbladder shapes and/or other body components of fish for use in subsequent *TS* modelling. Examples of these include investigations on Atlantic cod (Foote and Francis, 2002), Atlantic herring (Fässler *et al.*, 2009), Pacific herring (*Clupea pallasii*; Gauthier and Horne, 2004), lavnun (*Mirogrex terraesanctae*; Horne *et al.*, 2000), Chilean jack mackerel (*Trachurus symmetricus murphyi*; Peña and Foote, 2008), walleye pollock (Hazen and Horne, 2004), Pacific hake (*Merluccius productus*; Henderson and Horne, 2007), orange roughy (*Hoplostethus atlanticus*; Macaulay, 2002), and alewife (*Alosa pseudoharengus*; Reeder *et al.*, 2004). For these species, *in situ* measurements of *TS* were available beforehand for comparison with the model results. Consequently, the primary aim was usually not to estimate new *TS*–*L* relationships solely from the model results. Some of the studies that had both modelled and measured *ex situ* or *in situ* estimates of *TS* available presented comparisons between these respective datasets (Foote, 1985; Foote and Traynor, 1988; Clay and Horne, 1994; McClatchie *et al.*, 1998; Hazen and Horne, 2004; Reeder *et al.*, 2004; Henderson and Horne, 2007). In general, most of these comparisons have shown good agreement between the modelled *TS* values and those measured by *ex situ* and *in situ* experiments. Solely model-based *TS*–*L* relationships have been applied for acoustic abundance estimation before: the Commission for the Conservation of Antarctic Marine Living Resources (CCAMLR) has adopted a *TS* for Antarctic krill (*Euphausia superba*) that is based on a backscattering model using the stochastic distorted-wave Born approximation (Demer and Conti, 2005; Conti and Demer, 2006). Similarly, recent acoustic estimates of southern blue whiting (*Micromesistius australis*) in New Zealand (2009–2011) were based on modelled *TS* (Dunford and Macaulay, 2006).

The use of a slope fixed to 20 in the *TS*–*L* relationship is not better or worse than using a slope fitted to the set of data available (McClatchie *et al.*, 2003). Furthermore, there are no set criteria by which to select a fixed or fitted slope. For the boarfish samples modelled here, the difference in *TS* between a fixed slope and a slope fitted to the data for each set of angle distributions was at most 1 dB for the angular distribution $N(90^\circ, 5^\circ)$ and less than 0.5 dB for the angular distribution $N(88.5^\circ, 14.5^\circ)$ over the length range modelled. Thus, the selection of either set of parameters will not substantially influence population estimates one way or the other. However, fisheries management dislikes ambiguity, so a range of evaluation criteria proposed by McClatchie *et al.* (2003) were applied to the boarfish data. Following McClatchie *et al.* (2003), there are four comparisons or tests by which to evaluate the slope. The first test is to verify the hypothesis that the slope of the *TS*–*L* regression is different from 20 by fitting a linear relationship between *TS* and $\log_{10}(L)$. A *t*-value is calculated as the ratio between the fitted slope minus 20, and the s.e. of the fitted relationship. For boarfish, the *t*-test showed that the slope of the fitted regression between *TS* and $\log_{10}(L)$ for boarfish (22.6; s.e. = 2.7) was not significantly different from 20 (Student's *t*-test, $t = 0.99$, $p = 0.34$). The second test examines the allometric slopes relating dorsal swimbladder surface areas (*A*) to fish lengths. McClatchie *et al.* (2003) found that these were typically steeper and deviated from the isometric case ($A = aL^b$, where $b = 1$) for those species that had *TS*–*L* relationships with slopes significantly different from 20. The relationship between the dorsal swimbladder surface area and the total fish length in boarfish was found not to be significantly different from the isometric case (Student's *t*-test, $t = 0.667$, $p = 0.511$). Assuming that the swimbladder is the dominant sound reflector, this suggests a relationship of *TS* that is proportional to L^2. However, the ratio of the swimbladder surface area to boarfish length squared (mean = 0.020; s.d. = 0.005) was significantly smaller than in those fish species observed by McClatchie *et al.* (2003) that had a $20 \log_{10}(L)$ relationship (mean = 0.032; s.d. = 0.003; Student's *t*-test, $t = -6.54$, $p = 0.002$). This may suggest that due to their particular morphology, scaling of the *TS*–*L* regression is different for boarfish and could deviate from the rule of scaling by L^2. Lastly, the assumption of proportional increase in *TS* with the square of the fish length (i.e. slope of 20), as postulated

by Love (1971), holds for some species but not for others and depends on variation in fish morphotypes. Unlike other previously radiographed fish species that mostly showed an elongated and thin swimbladder, such as cod, alewife, Chilean jack mackerel, or herring (Foote and Francis, 2002; Reeder *et al.*, 2004; Peña and Foote, 2008; Fässler *et al.*, 2009), the boarfish has a relatively bulky and short swimbladder with a large circumference (Figures 2 and 3). Additionally, with the majority of adults being within the size range of ~12–17 cm (Hüssy *et al.*, 2012), boarfish are shorter than most of the species previously investigated. Thus, it is difficult to extrapolate from these established relationships using a fixed slope of 20 to boarfish based on morphometry. While not unanimous, the quantitative criteria support our recommendation of a TS–L relationship with the slope fixed to 20 for boarfish [$TS = 20\log_{10}(L) - 66.2$], at least until data suggest otherwise.

The modelling results of backscatter relative to fish tilt angle for a range of frequencies showed two distinctive features: (i) there was a very low directivity associated with the lower frequencies used (including 38 kHz); and (ii) the tilt angle that results in maximum backscatter becomes lower (head down direction) with increasing frequency. These features may reflect an increasing shift in importance from the swimbladder volume to the actual swimbladder surface shape at higher ratios between L and acoustic wavelength (λ) (Horne, 2000). Consequently, at high L/λ, the straight and flat parts of the swimbladder surface will cause enhanced backscatter when insonified at angles perpendicular to the incident wave front (Foote, 1980). This was observed at tilt angles of ~75° and ~110°, representing the aspect angle of the two distinct straight anterior and posterior parts of the dorsal swimbladder surface (Figure 3). In a previous investigation on TS of Chilean jack mackerel, Peña and Foote (2008) also observed maximum TS at 38 kHz at tilt angles less than 10° from dorsal incidence. They attributed this to different inclination angles relative to the fish axis along the swimbladder dorsal surface. Another factor additionally enhancing this effect may be the fish body, which increasingly contributes to the total TS at higher frequencies. The plateau seen in the 38-kHz TS curve for tilt angles between ~78° and 92° (Figure 4) should be advantageous, because tilt will have less of an effect on TS over a fairly broad tilt angle distribution. This facilitates surveying boarfish over broader periods (day, night, crepuscular), which for most fish species are usually associated with changes in behaviour, resulting in variations in the mean TS (Huse and Ona, 1996; Hazen and Horne, 2003). Moreover, boarfish swimbladders had similar width and height dimensions, making any potential bias due to roll angle deviations negligible. Tilt angle directivity can have a severe effect on TS in cases where the swimbladder has an elongated shape. Jech (2011) modelled the directivity pattern for Atlantic herring and showed that even at tilt angles $\pm 30°$ off horizontal orientation, TS at 38 kHz can be 25 dB (factor of ~300) less than the maximum value. For boarfish, this difference was ~6 dB (factor of ~4), making the effect of angle on TS comparably far less severe. The shift in tilt angle of the maximum TS value with increasing acoustic frequency also had an effect on the $r(f)$ and hence the acoustic identification properties of boarfish. Common with other investigations on multifrequency backscattering properties of physoclist species, the boarfish showed a decrease in $r(f)$ from 38 kHz towards higher frequencies. Pedersen and Korneliussen (2009) found that the rate of this decrease is primarily dependent on the typical average size of the fish species. In that respect, the boarfish $r(f)$ values shown here were comparable with those reported by Pedersen and Korneliussen (2009) for Norway pout (*Trisopterus esmarkii*), another small-bodied physoclist species. Given this physoclist frequency response exhibited by boarfish, there is potential to separate them from species that have different backscattering properties with the use of multifrequency acoustic methods (Horne, 2000; Kloser *et al.*, 2002; Korneliussen and Ona, 2003; Fässler *et al.*, 2007; Korneliussen *et al.*, 2009). Especially for Atlantic mackerel, which shows an increasing trend in $r(f)$ from 38 kHz towards 200 kHz (Gorska *et al.*, 2005, 2007; Korneliussen, 2010) and co-occurs with boarfish in space and time, possible acoustic discrimination may be beneficial during both survey (e.g. facilitated scrutinising) and fishing operations (e.g. avoiding bycatch).

A factor that affected the modelled mean TS was the choice of tilt angle distribution. Fish behaviour, reflected in the distribution of tilt angles within an aggregation of fish, is the most important factor influencing TS and hence the accuracy of subsequent abundance estimates using acoustic techniques (Foote, 1980; Hazen and Horne, 2003). The tilt angle distributions used in the averaging operations here have been applied widely for modelling backscatter of pelagic and semi-pelagic species but do not necessarily reflect the specific energetic requirements of the boarfish in the survey area. Only a limited quantity of *in situ* tilt angle measurements has been reported for pelagic species (Foote, 1980; McClatchie *et al.*, 1996). Tilt angle distributions observed for physoclists are generally normally distributed with means close to 90° (e.g. 89.1°; Foote and Ona, 1987) and various s.d. ranging between ~5° (e.g. 5.4°; Foote and Ona, 1987) and close to 20° (e.g. 17.4°; Olsen, 1971). The justification for the tilt angle distribution used in this study [i.e. $N(88.5°, 14.5°)$], to derive and recommend a TS–L relationship of the standard form, was to make use of the most elaborate and applicable tilt angle measurements currently available. These are based on measured and previously used distributions for swimbladder-bearing schooling pelagic species such as capelin, Atlantic herring, and cod. The means ranged from −4.4° to +3.8° relative to normal horizontal aspect, whereas the s.d. ranged from 10.3° to 18.4°, indicating a close-to-horizontal average orientation distribution with s.d. of ~15°. This is in agreement with a review by McClatchie *et al.* (1996) who looked at tilt angle distributions of a number of pelagic and semi-demersal species in different environments and found modes of around 90° for the mean and 15° for the s.d. Further, based on their observations, McClatchie *et al.* (1996) concluded that a Gaussian distribution with s.d. of ~15 should be used to average target strengths for use in acoustic surveys if no measurements are available. This is also consistent with previous studies that presented tilt angle averaged TS using a normal distribution with these characteristics (Gauthier and Horne, 2004; Hazen and Horne, 2004). Although the model-based TS–L relationship for boarfish presented here is based on parameters supported by the literature that are deemed most applicable in the absence of any more suitable information, there is still a lack of knowledge of behaviour of the boarfish. Given the importance of fish orientation distribution when modelling TS, future model estimates of TS for boarfish should make use of detailed tilt angle measurements on that species.

Acknowledgements

The biological sampling and radiography work was funded by the Killybegs Fishermen's Organisation (KFO; Killybegs, Co. Donegal, Ireland). SMMF received funding through the Dutch KBWOT Fisheries Programme for the project "Underpinning Acoustics" (KB-14-012-009-IMARES). Four anonymous reviewers provided valuable comments on a previous version of this manuscript.

References

Blanchard F., and Vandermeirsch F. 2005. Warming and exponential abundance increase of the subtropical fish *Capros aper* in the Bay of Biscay (1973-2002). Comptes Rendus Biologies, 328: 505–509.

Blaxter J. H. S., and Batty R. S. 1990. Swimbladder "behaviour" and target strength. Rapports et Procès-Verbaux des Réunions du Conseil International pour l'Exploration de la Mer, 189: 233–244.

Buerkele U. 1983. First look at herring distributions with a bottom referencing underwater towed instrumentation vehicle "Brutiv". FAO Fisheries Reports, 300: 125–130.

Carscadden J. E., and Miller D. S. 1980. Estimates of tilt angle of capelin using underwater photographs. ICES Document CM 1980/H: 50.

Clay C. S., and Horne J. K. 1994. Acoustic models of fish—the Atlantic cod (*Gadus morhua*). Journal of the Acoustical Society of America, 96: 1661–1668.

Clay C. S., and Medwin H. 1977. Acoustical Oceanography: Principles and Applications. Wiley, New York.

Conti S. G., and Demer D. A. 2006. Improved parameterization of the SDWBA for estimating krill target strength. ICES Journal of Marine Science, 63: 928–935.

Demer D. A., and Conti S. G. 2005. New target-strength model indicates more krill in the Southern Ocean. ICES Journal of Marine Science, 62: 25–32.

Dunford A. J., and Macaulay G. J. 2006. Progress in determining southern blue whiting (*Micromesistius australis*) target strength: results of swimbladder modelling. ICES Journal of Marine Science, 63: 952–955.

Fässler S. M. M. 2010. Target strength variability in Atlantic herring (*Clupea harengus*) and its effect on acoustic abundance estimates. PhD thesis, University of St Andrews, UK.

Fässler S. M. M., Fernandes P. G., Semple S. I. K., and Brierley A. S. 2009. Depth-dependent swimbladder compression in herring *Clupea harengus* observed using magnetic resonance imaging. Journal of Fish Biology, 74: 296–303.

Fässler S. M. M., Santos R., Garcia-Nunez N., and Fernandes P. G. 2007. Multifrequency backscattering properties of Atlantic herring (*Clupea harengus*) and Norway pout (*Trisopterus esmarkii*). Canadian Journal of Fisheries and Aquatic Sciences, 64: 362–374.

Fish M. P. 1948. Sonic Fishes of the Pacific. Woods Hole Oceanographic Institution, Woods Hole, MA.

Foote K. G. 1980. Averaging of fish target strength functions. Journal of the Acoustical Society of America, 67: 504–515.

Foote K. G. 1983. Linearity of fisheries acoustics, with addition theorems. Journal of the Acoustical Society of America, 73: 1932–1940.

Foote K. G. 1985. Rather-high-frequency sound scattering by swimbladdered fish. Journal of the Acoustical Society of America, 78: 688–700.

Foote K. G. 1987. Fish target strengths for use in echo integrator surveys. Journal of the Acoustical Society of America, 82: 981–987.

Foote K. G., and Francis D. T. I. 2002. Comparing Kirchhoff-approximation and boundary-element models for computing gadoid target strengths. Journal of the Acoustical Society of America, 111: 1644–1654.

Foote K. G., and Ona E. 1987. Tilt angles of schooling penned saithe. Journal du Conseil International pour l'Exploration de la Mer, 43: 118–121.

Foote K. G., and Traynor J. J. 1988. Comparison of walleye pollock target strength estimates determined from *in situ* measurements and calculations based on swimbladder form. Journal of the Acoustical Society of America, 83: 9–17.

Gauthier S., and Horne J. K. 2004. Acoustic characteristics of forage fish species in the Gulf of Alaska and Bering Sea based on Kirchhoff-approximation models. Canadian Journal of Fisheries and Aquatic Sciences, 61: 1839–1850.

Gorska N., Korneliussen R. J., and Ona E. 2007. Acoustic backscatter by schools of adult Atlantic mackerel. ICES Journal of Marine Science, 64: 1145–1151.

Gorska N., Ona E., and Korneliussen R. 2005. Acoustic backscattering by Atlantic mackerel as being representative of fish that lack a swimbladder. Backscattering by individual fish. ICES Journal of Marine Science, 62: 984–995.

Harden Jones F. R., and Marshall N. B. 1953. The structure and function of the teleostean swimbladder. Biological Reviews, 28: 16–83.

Harden Jones F. R., and Scholes P. 1981. The swimbladder, vertical movements and the target strength of fish. *In* Meeting on Hydroacoustical Methods for Estimation of Marine Fish Populations, 25–29 June 1979. 2. Contributed Papers, Discussion and Comments, pp. 157–181. The Charles Stark Draper Laboratory Inc., Cambridge, MA.

Hazen E. L., and Horne J. K. 2003. A method for evaluating the effects of biological factors on fish target strength. ICES Journal of Marine Science, 60: 555–562.

Hazen E. L., and Horne J. K. 2004. Comparing the modelled and measured target-strength variability of walleye pollock, *Theragra chalcogramma*. ICES Journal of Marine Science, 61: 363–377.

Henderson M. J., and Horne J. K. 2007. Comparison of *in situ*, *ex situ*, and backscatter model estimates of Pacific hake (*Merluccius productus*) target strength. Canadian Journal of Fisheries and Aquatic Sciences, 64: 1781–1794.

Horne J. K. 2000. Acoustic approaches to remote species identification: a review. Fisheries Oceanography, 9: 356–371.

Horne J. K., and Jech J. M. 1999. Multi-frequency estimates of fish abundance: constraints of rather high frequencies. ICES Journal of Marine Science, 56: 184–199.

Horne J. K., Walline P. D., and Jech J. M. 2000. Comparing acoustic model predictions to *in situ* backscatter measurements of fish with dual-chambered swimbladders. Journal of Fish Biology, 57: 1105–1121.

Huse I., and Ona E. 1996. Tilt angle distribution and swimming speed of overwintering Norwegian spring spawning herring. ICES Journal of Marine Science, 53: 863–873.

Hüssy K., Coad J. O., Farrell E. D., Clausen L. W., and Clarke M. W. 2012. Sexual dimorphism in size, age, maturation, and growth characteristics of boarfish (*Capros aper*) in the Northeast Atlantic. ICES Journal of Marine Science, in press.

ICES. 2011. Report of the Working Group on Widely Distributed Stocks (WGWIDE). ICES Document CM 2011/ACOM: 15. 642 pp.

Jech J. M. 2011. Interpretation of multi-frequency acoustic data: effects of fish orientation. Journal of the Acoustical Society of America, 129: 54–63.

Jech J. M., and Horne J. K. 1998. Sensitivity of acoustic scattering models to fish morphometry. Proceedings of the 135th Meeting of the Acoustical Society of America, Seattle, 20–26 August 1998, pp. 1819–1820.

Kloser R. J., Ryan T., Sakov P., Williams A., and Koslow J. A. 2002. Species identification in deep water using multiple acoustic frequencies. Canadian Journal of Fisheries and Aquatic Sciences, 59: 1065–1077.

Korneliussen R. J. 2010. The acoustic identification of Atlantic mackerel. ICES Journal of Marine Science, 67: 1749–1758.

Korneliussen R. J., Heggelund Y., Eliassen I. K., and Johansen G. O. 2009. Acoustic species identification of schooling fish. ICES Journal of Marine Science, 66: 1111–1118.

Korneliussen R. J., and Ona E. 2003. Synthetic echograms generated from the relative frequency response. ICES Journal of Marine Science, 60: 636–640.

Love R. H. 1971. Dorsal-aspect target strength of an individual fish. Journal of the Acoustical Society of America, 49: 816.

Macaulay G. J. 2002. Anatomically detailed acoustic scattering models of fish. Bioacoustics, 12: 275–277.

MacLennan D. N. 1992. Fishing gear selectivity—an overview. Fisheries Research, 13: 201–204.

MacLennan D. N., Fernandes P. G., and Dalen J. 2002. A consistent approach to definitions and symbols in fisheries acoustics. ICES Journal of Marine Science, 59: 365–369.

MacLennan D. N., and Menz A. 1996. Interpretation of *in situ* target-strength data. ICES Journal of Marine Science, 53: 233–236.

Marshall N. B. 1960. Swimbladder structure of deep-sea fishes in relation to their systematics and biology. Discovery Reports, 31: 3–122.

McClatchie S., Alsop J., and Coombs R. F. 1996. A re-evaluation of relationships between fish size, acoustic frequency, and target strength. ICES Journal of Marine Science, 53: 780–791.

McClatchie S., Macaulay G., Hanchet S., and Coombs R. F. 1998. Target strength of southern blue whiting (*Micromesistius australis*) using swimbladder modelling, split beam and deconvolution. ICES Journal of Marine Science, 55: 482–493.

McClatchie S., Macaulay G. J., and Coombs R. F. 2003. A requiem for the use of 20 log(10) length for acoustic target strength with special reference to deep-sea fishes. ICES Journal of Marine Science, 60: 419–428.

Medwin H., and Clay C. S. 1998. Fundamentals of Acoustical Oceanography. Academic Press, Boston.

O'Donnell C., Farrell E. D., Nolan C., and Campbell A. 2012. Boarfish Acoustic Survey Cruise Report. 2012/03 Marine Institute, Galway, Ireland. http://hdl.handle.net/10793/822.

O'Donnell C., Farrell E. D., Saunders R. A., and Campbell A. 2011. Boarfish Acoustic Survey Cruise Report. 2011/03 Marine Institute, Galway, Ireland. http://hdl.handle.net/10793/675.

Olsen K. 1971. Orientation measurements of cod in Lofoten obtained from underwater photographs and their relation to target strength. ICES Document CM 1971/B: 17.

Ona E. 1984. Tilt angle measurements on herring. ICES Document CM 1984/B: 19.

Ona E. 2001. Herring tilt angles measured through target tracking. *In* Herring: Expectations for a New Millennium, pp. 461–487. Lowell Wakefield Fisheries Symposium, 18.

Pedersen G., and Korneliussen R. J. 2009. The relative frequency response derived from individually separated targets of northeast Arctic cod (*Gadus morhua*), saithe (*Pollachius virens*), and Norway pout (*Trisopterus esmarkii*). ICES Journal of Marine Science, 66: 1149–1154.

Peña H., and Foote K. G. 2008. Modelling the target strength of *Trachurus symmetricus murphyi* based on high-resolution swimbladder morphometry using an MRI scanner. ICES Journal of Marine Science, 65: 1751–1761.

Reeder D. B., Jech J. M., and Stanton T. K. 2004. Broadband acoustic backscatter and high-resolution morphology of fish: measurement and modeling. Journal of the Acoustical Society of America, 116: 747–761.

Simmonds E. J., and MacLennan D. N. 2005. Fisheries Acoustics: Theory and Practice. Blackwell Science, Oxford.

Soule M., Barange M., and Hampton I. 1995. Evidence of bias in estimates of target strength obtained with a split-beam echo-sounder. ICES Journal of Marine Science, 52: 139–144.

Yasuma H., Sawada K., Ohshima T., Miyashita K., and Aoki I. 2003. Target strength of mesopelagic lanternfishes (family Myctophidae) based on swimbladder morphology. ICES Journal of Marine Science, 60: 584591.

Yasuma H., Sawada K., Takao Y., Miyashita K., and Aoki I. 2010. Swimbladder condition and target strength of myctophid fish in the temperate zone of the Northwest Pacific. ICES Journal of Marine Science, 67: 135–144.

Handling editor: David Demer